The interaction of bulk heterojunction donor/acceptor blends with polaritonic state creation in organic crystalline films

By Reid Center

An undergraduate thesis advised by Dr. Oksana Ostroverkhova

Submitted to the Department of Physics, Oregon State University

in partial fulfillment of the requirements for the degree BSc in Physics

Submitted on 5/29/20

Abstract:

We explore the interactions between charge transfer exciton states (CTEs) and an optical microcavity by testing the effects that cavity resonance has on the CTEs and if CTEs can be coupled with a photon to create quasiparticles known as polaritons. Exciton polaritonics is becoming a booming area of research mainly due to the variety of intriguing consequences of these quasiparticles. Here, we specifically look into how the environment can affect the creation of exciton polaritons in organics. To do this, we fabricated optical microcavities and placed a thin film of a functionalized Anthradithiophene derivative inside the cavity. The transmitted photoluminescence was measured at varying angles off of the cavity's surface normal to gather spectra. Using the maximum energies of these peaks, we model the energies with respect to angle of detection. In this way, one can demonstrate Rabi splitting, thus verifying the existence of polaritons. Our data shows no Rabi splitting in a cavity that matches resonances with the CTEs, but that polaritons can form with the Frenkel exciton state when cavity resonance matches that of the Frenkel exciton. The combination of these phenomena is intriguing as it offers pathways to reduce CTEs creation in devices as well as the possibility of discovering a new form of polariton.

Table of Contents:

Introduction:

1.1 Motivation

The field of polaritonics has been greatly influenced by the addition of organics. The ability to create excitons at room temperature gives organics a leg up on the competition and at a low cost of production and environmentally friendly, organic semiconductors have offered a plethora of opportunities. Organics are solution processible and can be easily deposited onto flexible substrates via liquid deposition. Another key feature that organics bring to the table is a tunable molecule. The backbone of the molecule can remain constant as side groups are changed in order to create different properties in the material such as variable colors and crystalline stacking structures. Quantum computing, low-threshold lasing, room temperature Bose-Einstein condensates, and medicine are current fields of interest and study in the world of polaritonics, but there is much that is unknown about polaritons in organic semiconductors and the unique properties that they possess.[1]

My project explores the interactions between Frenkel and charge transfer states and cavity photons by placing an acceptor/donor blend of semiconductors inside a Fabry-Perot optical micro-cavity. The main goal of this project is to fabricate cavities that resonate at conducive frequencies for coupling to the CTEs and to determine if polaritons can be created by coupling to an exciton shared over two molecules.

1.2 Excitons

Standard semiconductors are defined as being a material that possesses an electric conductivity value between that of a conductor and that of an insulator. Classically, a semiconductor will absorb a photon and use the energy to promote an electron from the valence band to the conduction band. In this case, the photon energy must exceed the energy of the band gap to promote an electron. If the system is cooled, however, exciton transitions can be seen at low energies. An exciton is a way to model an excited electron that is not completely freed from the Coulomb interaction between the electron and the potential well that it left behind. The exciton transition energy is lower than that of the bandgap and thus doesn't allow the electron to escape from the potential well. The pairing of the electron and hole can be treated as a single particle that maintains momentum dependence. Excitons are what's known as a quasi-particle, as it is actually a combination of an excited electron and the potential well that it leaves behind known as a hole. The exciton is a coulomb-bounded electron-hole pairing. The attractive force is represented by equation 1,

$$\frac{-e^2}{\epsilon * r^2} \tag{1}$$

Here, epsilon represents the dielectric constant, e is the charge of an electron, r is the distance between the electron and hole, and the energy is proportional to one over epsilon.[2]

Excitons are difficult to form at room temperature in classic semiconductors, as the dielectric constant of standard semiconductors is high, causing a small binding energy and

attraction force. This requires one to cool down their system to lower than band gap energy to observe exciton emission.

On the contrary, in organic semiconductors, the dielectric constant is much lower, around 3~3.5, causing a much stronger binding force.[3] This allows us to see exciton formation at room temperature. When we do this, one is still well below the band gap energies and we do not see these transitions.

This is the base particle that we use and alter in this project. It is the groundwork for the excimer and polaritonic states that I am working with.

1.3 Exciplex

The term excimer refers to an excited dimeric state that exists between two molecules[4]. Simply put, our exciton is now living on two different molecules. Exciplex is a specific type of excimer that is heterodimeric and is thus formed between two different species of molecules, as opposed to a normal dimeric excimer that is formed between two molecules of the same species. This is a special bound state that can only exist in an excited state as the two molecules will not form a dimeric state if left in the ground state. Donor molecules that fluoresce in the region that acceptor molecules absorb tend to make the best donor/acceptor pairs. The donor/acceptor molecule's photoluminescence vs. absorption are shown in Figure 1, which is taken from one of our group's previous publications, [5].

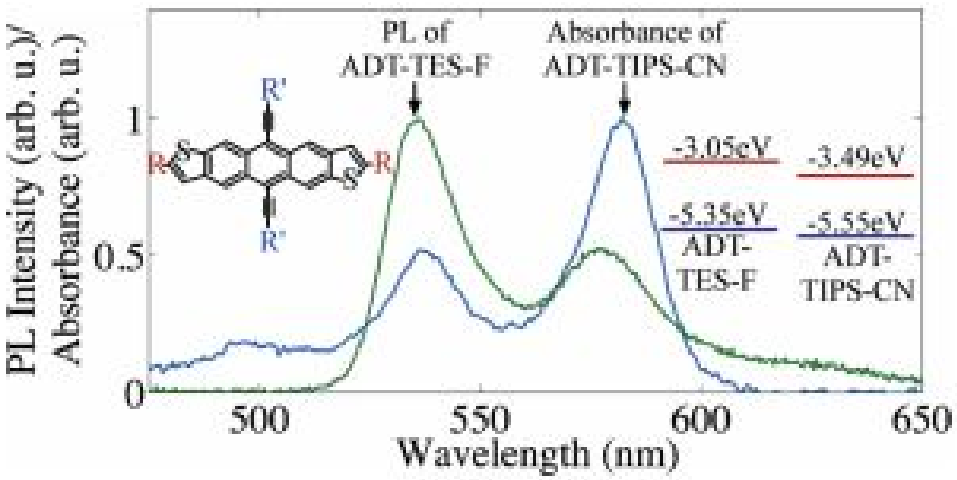

Figure 1: Absorbance of the acceptor molecule ADT-TIPS-CN and the Photoluminesence of our donor ADT-TES-F in toluene solution. The molecular structure is shown on the left. HOMO and LUMO levels are shown to the right of the spectra. Side group locations, TES and TIPS, are represented by R' while R represents end groups of either F or CN. From Ref. [5]

The quantum mechanics of the creation of an excimer state is a two step process. The molecules start in their ground state H.O.M.O. (highest occupied molecular orbital), and are then excited as light is absorbed. The molecule with a higher L.U.M.O. (lowest unoccupied molecular orbital) level, absorbs the photon and elevates an excited electron into the L.U.M.O. level, thus populating the L.U.M.O. energy level. This creates a standard exciton. The exciton now has a number of ways to decay. It can decompose in non-fluorescent or fluorescent processes. In this case, both types of state relaxation are occuring. There are two paths that are energetically preferable. The exciton can relax normally by recombining the electron/hole pair and fluorescing in that molecule's normal photoluminescence spectra, or the excited electron can cross into the L.U.M.O level of the nearby molecule, creating an excited bound state referred to as charge transfer exciton state, CTEs.

Another way to think of the recombination process is that the hole of the exciton remains on the donor molecule while the excited electron transfers to the acceptor molecule, thus binding the two molecules as the exciton spans the two molecules. This CTEs then decomposes and fluorescence can be seen in between the peaks of the donor and acceptor molecule as can be seen in figure 2[5].

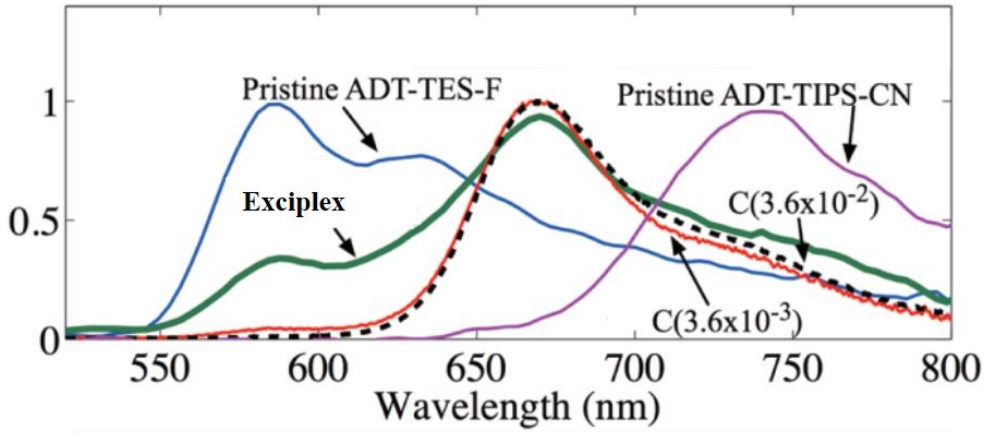

Figure 2: Exciplex emission peak shown in between emission peaks from pristine films of the donor, ADT-TES-F, and acceptor, ADT-TIPS-CN, molecules. Taken from a previous publication by our group. From Ref. [5]

CTEs are very long lived in comparison to other excited state lifetimes, increasing the excited state lifetime by a factor of four or higher. This makes them especially exciting for use in organic photovoltaics.[6] CTEs can be used to generate current by placing an electric potential over the molecules. If the voltage is strong enough, this can separate the hole and electron pairing by ripping the bounded state apart. The efficiency of these solar cells is based on how tightly bound the electron is to the hole; the lower the binding energy, the higher the efficiency will be.

Exciplex states are a subset of CTEs that are tightly bound. For this reason, exciplex states can be problematic for these D/A solar cells as this makes it difficult to separate the charges from their potential wells[6]. If the electron is bound too tightly to the potential well, the electron will simply relax back to a lower energy state, thus ruining a device's ability.

CTEs are also exciting as they exhibit static electric dipole moments[7]. A possible application would allow for manipulation of the quasi-particle via electrical fields and is an ongoing field of study[8]. Currently, the field of theoretical organic semiconductors has yet to formally examine the interactions between CTEs and polaritonic states. One question that remains unanswered is whether or not one can use polaritons to reduce the binding energy of the exciplex to make it more useful in solar cells or other optoelectronic devices.

1.4 Exciton Polaritons

Exciton polaritons are a quasiparticle created by the strong coupling between a bound E-field mode and an exciton, though, polaritons can be created by coupling a photon to other electric dipoles, such as surface plasmons or phonons as well.

Polariton energy states are created by making a resonant cavity out of reflective conductors. This creates boundary conditions for the E-field. The energy of the bound mode is based on how thick the cavity is and the effective index of refraction of the active layer inside the cavity. The resonance of the cavity determines the wavelength of light that becomes trapped inside the cavity. This standing wave that has been trapped inside our cavity can then interact with the dipole moment of an exciton. The coupling of light to matter is usually quite weak as

the wavelength of light is far greater than the size of an atom, but a Fabry-Perot microcavity allows light with energy near the exciton absorption transition to strongly couple to the exciton.

The interaction between a photon and this environment causes the photon to increase in energy as the angle of the incident light increases.[9] The parameter for maximum constructive interference in a Fabry Perot optical cavity is for the perpendicular element of the incident light's K vector to be half a wavelength, thus granting the lowest normal mode for the light to couple with the cavity. As the angle increases, the K vector must increase to maintain this maximum constructive interference. The K vector is proportional to energy and thus, as the K vector of the photon increases, so too must the energy. This causes a blue shifting of the spectra as the angle of the incident light increases.

The observation of a polariton can be confirmed when Rabi splitting can be observed. Rabi splitting is derived from the coupled harmonic oscillator model. This presents us with equation 2.[10]

$$\begin{bmatrix} E_p & V \\ V & E_x \end{bmatrix} \begin{bmatrix} \alpha \\ \beta \end{bmatrix} = \mathrm{E} \begin{bmatrix} \alpha \\ \beta \end{bmatrix} \tag{2}$$

Here, E_p and E_x are the photon and exciton transition energies respectively, with V representing the coupling coefficient, and α and β equaling eigenvector mixing coefficients. The eigenvalues of this matrix give rise to a splitting in the energy regime when E_p and E_x are equivalent to each other. This effect is shown in Figure 3.

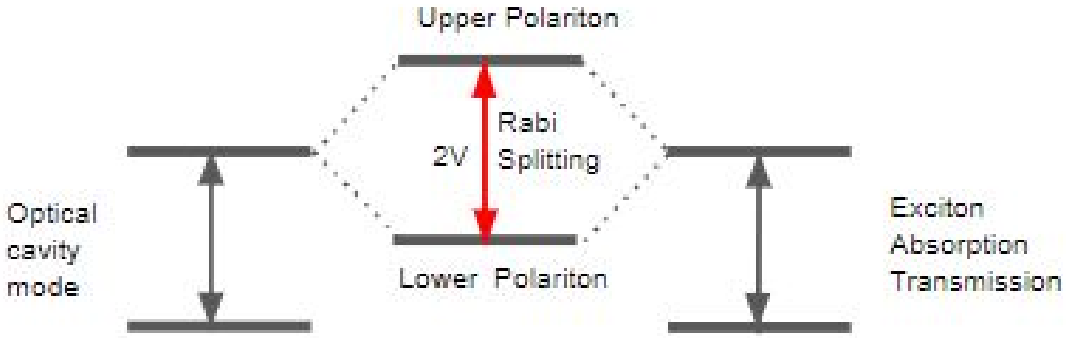

Figure 3: Polariton energy levels splitting when the energies of the coupled oscillators become equivalent and thus indistinguishable. Rabi splitting equalling twice the coupling coefficient V.

This gives a Rabi splitting effect and shows the first two polariton energy states, known as the upper and lower polariton energy states. The angle of the incident light changes the resonant energy of the cavity because the magnitude of the K vector interacts with the resonant mode of the cavity and locks it into a specific mode[10]. The energies, seen in Figure 4, can be plotted over the angle of detection to create a plot of the Rabi splitting, which will be equivalent to twice the coupling coefficient V. We will be taking data and matching it against this graph to determine if polaritons are forming in our cavities.

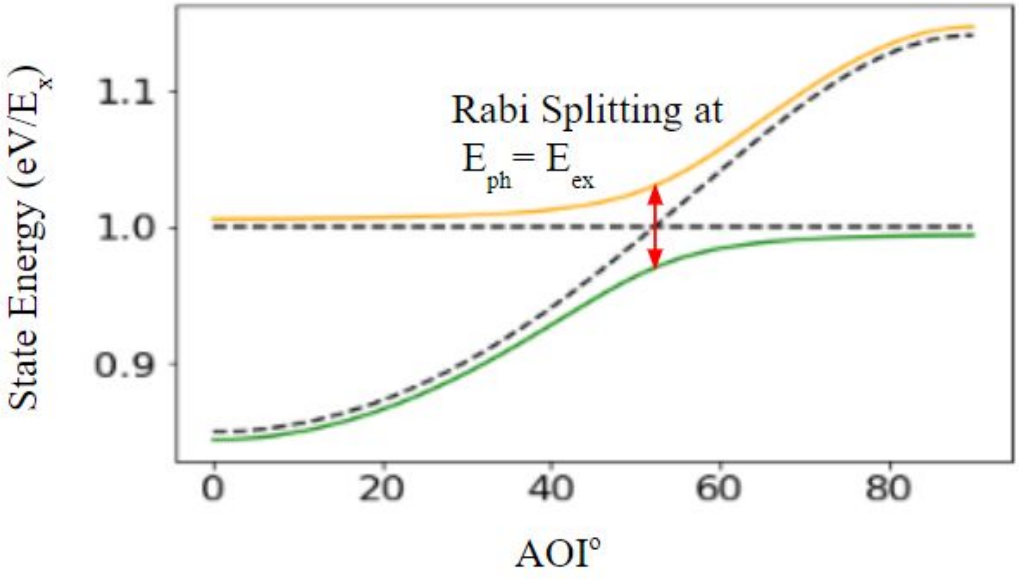

Figure 4: The Rabi splitting of the first two polaritonic states occurs when the energies of the exciton, horizontal line, and photon, dotted curve, become equal in value. The difference in energy is 2 V at this point.

This area of research is not based on a specific theoretical prediction of polaritonic activity, and is more targeted at exploring the interactions experimentally. The answer to the question of how these particles interact with exciplex states is the primary goal of this thesis.

Methods:

2.1 Sample Prep

The project began with the goal of creating an ADT donor/acceptor solution in toluene of a concentration such that the molecular spacing between molecules was between 5-10 nm. Equation 3 shows the equation for determining the distance between molecules in solution /film.[10]

$$V = \frac{4\pi}{3}\left(\frac{d}{2}\right)^3 \quad (3)$$

Here, V is equivalent to the volume per molecule and d is the distance between molecules. The further derivation was taken from David Haas' thesis[10] and results in a total distance formula shown in equation 4.

$$d = 0.644\ \text{nm}\ \sqrt[3]{f}. \quad (4)$$

Here, f is the mole ratio of the PMMA solution over the ADT solution. The different ADT species were treated as one for this calculation. This derivation remains valid as the molecular weights used to calculate this equation are the same that I am using.

Multiple solutions of already made ADT were available, but they were solutions made of a single ADT derivative and their concentrations were unknown. We evaporated all of the solvent off of the old solutions by a combination of heat and increased air circulation over the solution by placing it on a hot plate in a fume hood while simultaneously blowing air over the surface. New solutions were made by adding a known amount of toluene to bring the new solution to a known volume. The solutions were then placed into a 1 cm cuvette, absorption taken via a tungsten-halogen lamp and the software Spectrasuite, and then diluted by a known amount, cutting the concentration roughly in half each dilution. This was done up to five times for each ADT derivative solution.

Absorption measurements were taken with a tungsten halogen lamp as a white light source with the cuvette housed in a homemade device that allowed for optical fibers to deliver and receive the light on either end of the cuvette. After determining the proper concentrations of each ADT solution, we mixed the final donor/acceptor solution to have 98% donor molecule, a fluorinated anthradithiophene derivative that has been functionalized with (TES), triethylsilylethynyl, side groups, or (diF TES-ADT), and 2% acceptor, (ADT-TIPS-CN), (triisopropylsilylethynyl) and (cyanine). PMMA, (Polymethyl methacrylate), was also added to create a 0.3 molar solution to aid in the smoothness of the films. The final solution was created with an intermolecular distance of around 1.8 nm for ADT molecules and as a 0.3 Molar solution with respect to PMMA. The data was gathered using a spectrometer and the program Spectrasuite. Once the analysis and creation of the semiconductor solution was complete, we spin cast the solution onto silvered glass slides with the silver layer being approximately 50nm thick[10]. We spin for one minute, the speed ranging from 800 rpm to 3200 rpm, increasing by 400 rpm per sample to create a variety of thicknesses of our active layer. This process allowed us to gain a range of thicknesses such that we could vary the resonance of our cavities. Then, the slides were “capped” by evaporating another 50 nm layer of silver on top of the semiconductor layer using an electron gun housed in a vacuum chamber with a band down the middle left uncapped for further analysis of the film.

2.2 Ellipsometry

To test the thickness of the samples, we used an ellipsometer in the Gibbons lab. Ellipsometry uses light to measure the change in polarization of light reflected off a thin film. This technique allows one to determine the thickness of a thin film as well as the index of refraction of the film. The thickness of the films determines the thickness of the cavity and thus the wavelength of cavity resonance. We used ellipsometry to determine if the samples would resonate at the proper wavelengths by using a premade model our lab had made previously to "cap" the sample with 50 nm of silver. The model determined that on the 800 rpm sample, the resonance would be around the 800-900 nm range. However, the 1200 rpm sample was modelled to resonate at a wavelength of 685 nm which is in a similar location to the peak of the exciplex emission. This means that equating the photon and exciton energies is possible and thus is where we expect to see coupling to our exciplex. The 1600 rpm sample model showed resonance around the peak of the isolated donor Frenkel exciton emission, which is roughly 530 nm. No further cavities were analyzed as the 1600 rpm cavity already overshot the targeted cavity thickness.

2.3 Measurements

After the samples were fabricated, angle resolved photoluminescence (PL) measurements were taken by shining a laser, 532 nm in this case, through the microscope's side port and off a beam splitter into the glass slide from underneath. This custom built, confocal, angle resolved, PL detection setup (Tower of Power, figure 5) allows for PL measurements to be taken from angles ranging from surface normal ranging from zero degrees to ninety. We took measurements between surface normal and 70 degrees in steps of 5 degrees. Measurements were taken at both P

and S polarized light, and a polarizer is built into the Tower of Power. The Tower of Power is mounted on top of our microscope (model: Olympus IX71), and has three degrees of freedom. S and P polarizations were taken from the same spot. Concern over photobleaching was rectified by testing the initial polarization and angle and testing the intensities before and after the measurements. The final intensity was slightly lower, however it was under five percent different and seeing as how this is not the focus of this thesis, effects of photobleaching are small enough to be negligible and are thus ignored.

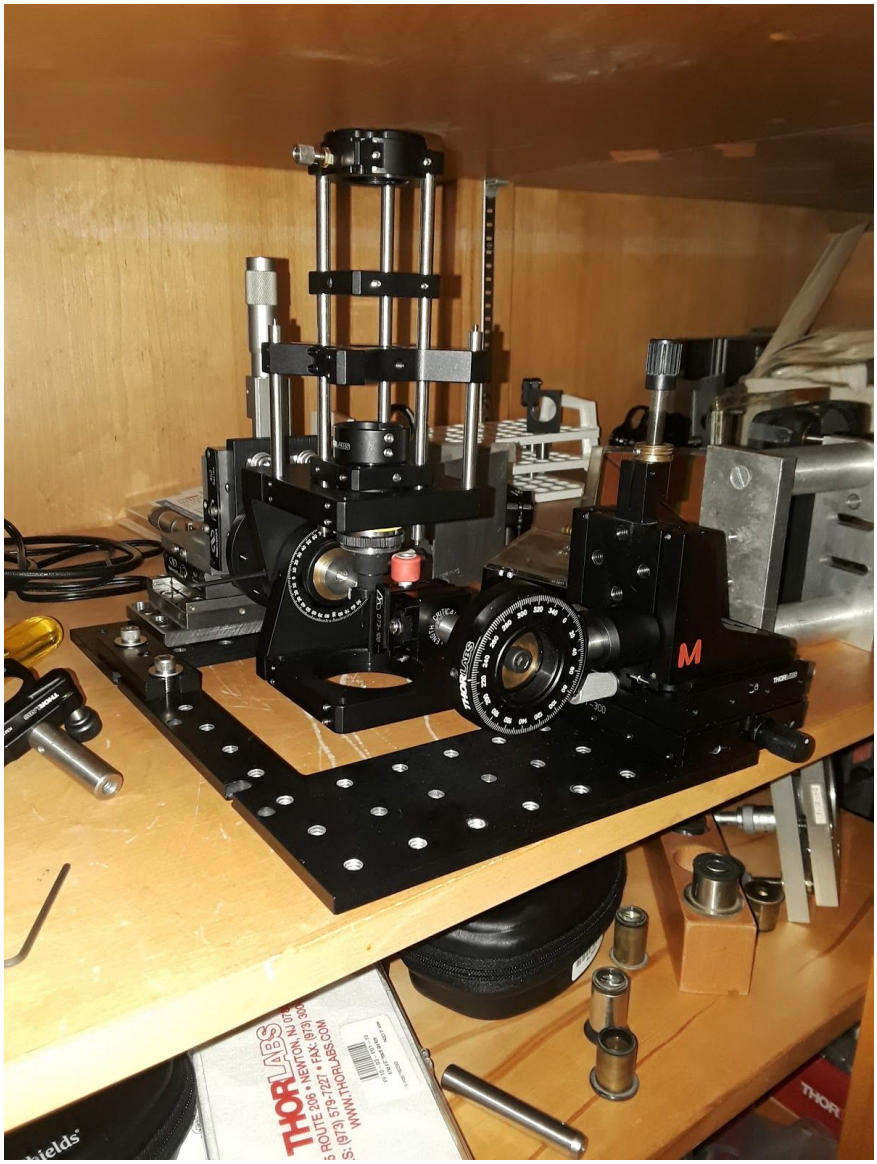

Figure 5.1: Tower of Power. Used to take angle resolved PL data at various angles off surface normal. ToP sits on top of the microscope when in use.

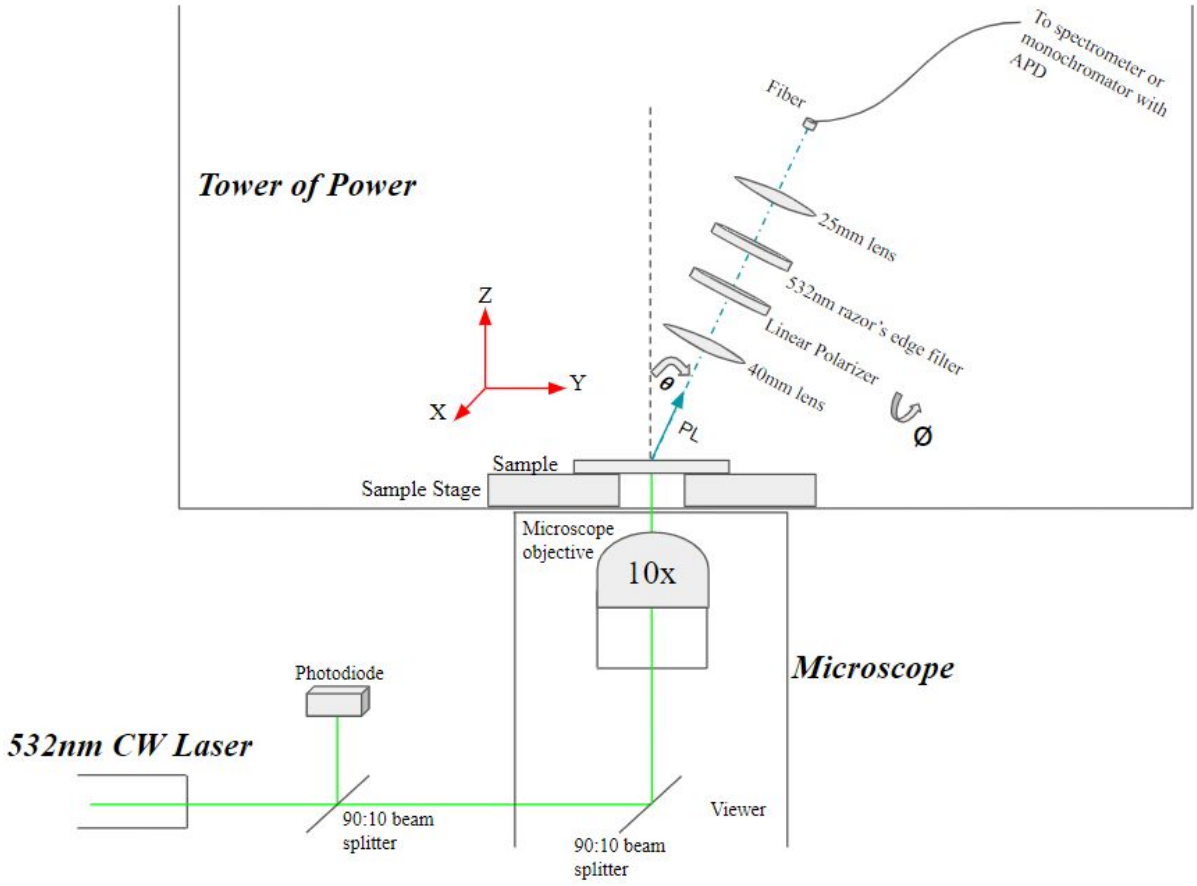

Figure 5.2: Schematic of entire experimental setup. A pulsed excitation laser can also be used as an input when one is taking excited lifetime measurements. The first beam splitter and photodiode serve this purpose. Output leads to either a spectrometer when gathering PL spectra or to a monochromator with an APD for taking banded excited state lifetime measurements.

2.4 Data Analysis

Data analysis was done using a variety of methods ranging from simple graphing techniques using pyplot software for graphing the absorption and PL spectra to the utilization of "scipy.optimize.curve_fit" as well as code that uses the least squares and maximum likelihood estimation methods for analysis of the histograms produced by our avalanche photodiode (APD) by curve fitting the various slopes in the model. All histogram analysis code can be found on

GitHub. The first analysis done was utilizing python to curve fit PL spectra with gaussians, allowing us to determine how many species of molecules exist in our sample. This was done using “scipy.optimize.curve_fit” and guessing the parameters, then using the previous peak as the parameter for the next curve. This strategy was looped over for each curve taken. The peak locations for each curve were then extracted and plotted vs the angle of incident that the spectrum was taken at. The resulting graph is now in the proper space to determine if polaritons exist in the sample by demonstrating a Rabi splitting.

Results/Discussion:

3.1 Exciplex Confirmation

PL from the uncovered films show a peak at approximately 667 nm, indicating exciplex formation as neither ADT-TES-F nor ADT-TIPS-CN have photoluminescence peaks at 667 nm . We succeeded in creating cavities that resonated around the fluorescence spectra of both the exciplex and the Frenkel exciton peaks as seen in Figure 6.

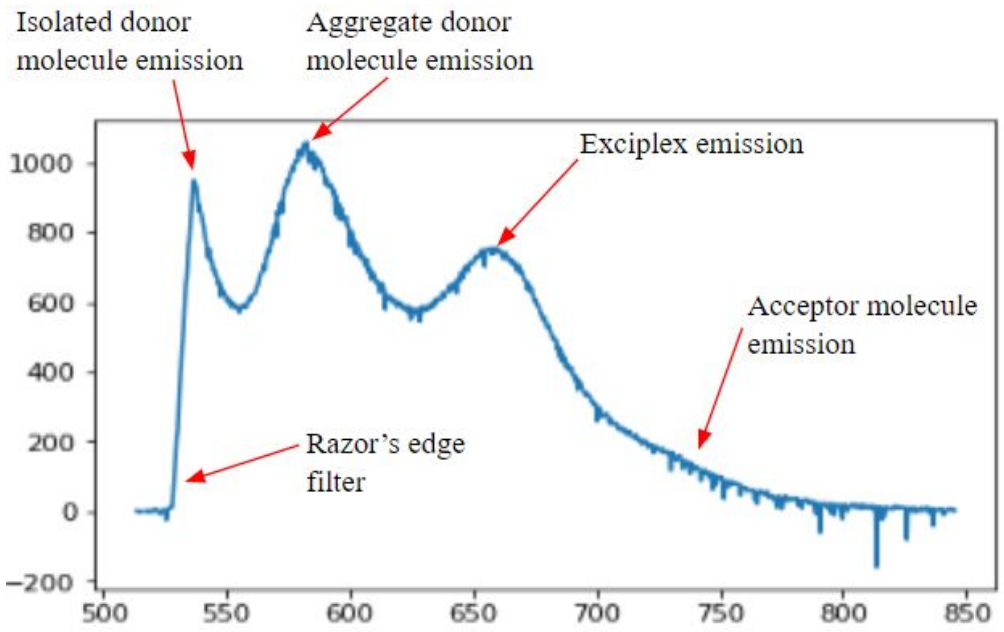

Figure 6: PL obtained off the uncapped section of Cavity 2. The solution used was 98% donor molecule and 2% acceptor molecule, explaining their difference in intensity between the aggregate donor emission and the acceptor emission.

This spectrum shows four peaks. The left side of the plot shows the razors edge filter at 532 nm to block the excitation laser. The peaks at ~530 nm and 580 nm correspond to emission from isolated ADT-TES-F molecules and ADT-TES-F aggregates respectively, *Shepherd et al., Appl Phys Lett 2010*.[11] The peak at ~670nm is the CTEs emission and is between the peaks of the donor and acceptor. Finally, a small ridge can be seen at a longer wavelength, showing the PL of the acceptor molecule. We compare this to Figure 2, and can see that all of the peaks are where we expect them to be. This measurement was taken before the final capping of the cavities, however exciplex emission can be seen in cavities that select for different wavelengths of light, so it is definitely happening inside the cavities.

3.2 Relevant Cavities

Seven cavities were created, however only a few were in the realm of interest. These are detailed in the following table.

Cavity ID	Cavity RPM	Surface Normal Resonant Wavelength
1	800	~900 nm
2	1200	~ 685 nm
3	1600	~ 590 nm
4	2000	Untested
5	2400	“.....”
6	2800	“.....”
7	3200	“.....”

Cavity one resonated at a range of wavelengths above our CTEs’ resonance and thus wasn’t analyzed further. Cavities 4-7 resonated below 532 nm. This was problematic due to the 532 nm laser excitation. Since we lacked equipment to fully analyze the rest of the created cavities, they will not be discussed further.

Out of the seven, two cavities were tested. Cavity two resonated at approximately the same wavelength as our exciplex wavelength. The PL was taken at surface normal to seventy degrees off surface normal in steps of 5 degrees. The curves are modeled in python and these plots are shown below.

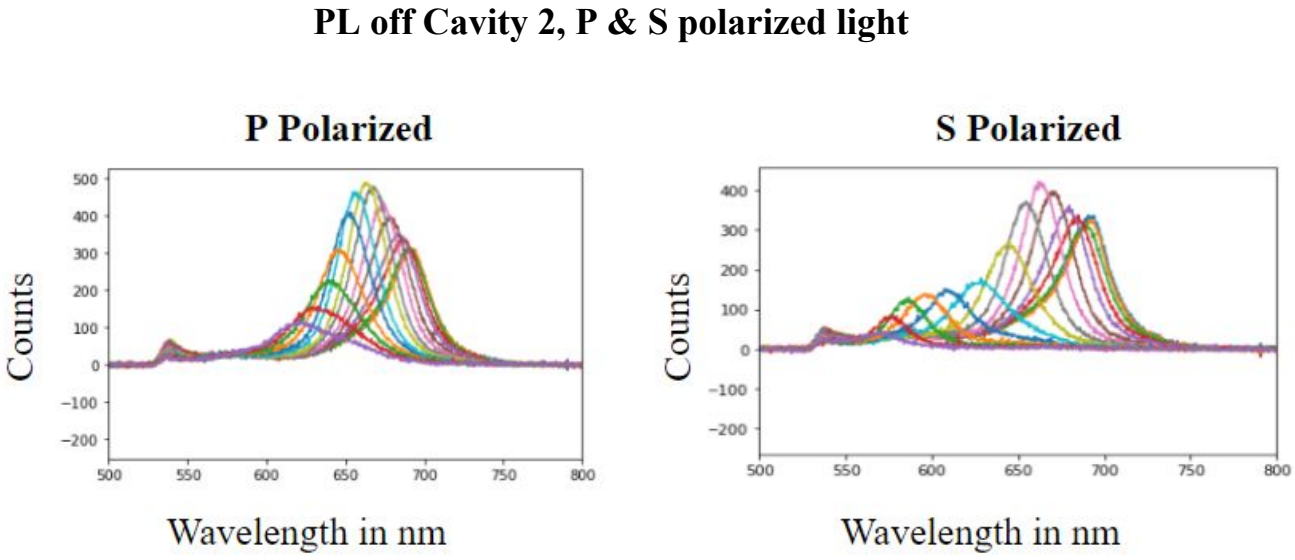

Figure 7.1: Polarized PL from Cavity 2. This resonance matches the emission from our CTEs. The right most curve is taken at surface normal, each increment of five degrees blue shifts the emission peak. 14 spectra were taken for each polarization at the same spot. The bump at 532 nm is bleedover from the laser.

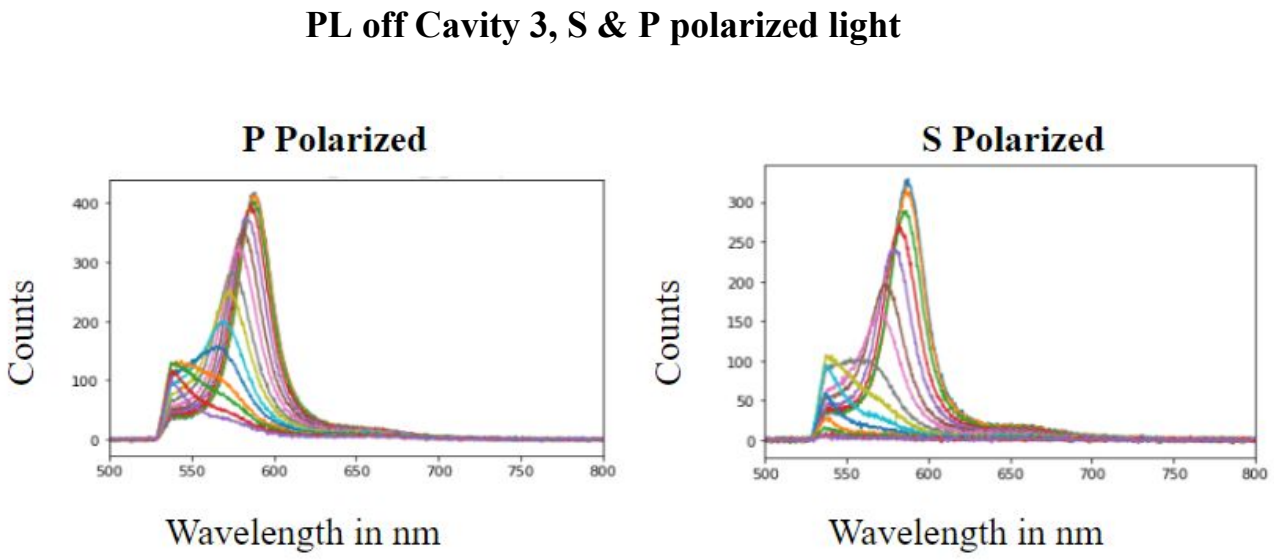

Figure 7.2: Polarized PL from Cavity 3. Here, the peaks blueshift through the razor's edge filter, but we use the projected peak locations that are based off of cavities one and two's behavior.

The location of the peak of each curve was then extracted and used to determine if Rabi splitting is happening.

3.3 Rabi Splitting

Analysis of the data was done in python. The code used the 'least squared' method of curve fitting. This was used on spectra from cavities one through three. This involves using a sum of gaussians to fit each peak shown in Figure 7. Doing this allows us to correct for the razor's edge filter in figure 7.2 to extract the true peak locations from our spectra.

Cavity one resonated in the 800 nm range, which is out of the range of wavelength in which one would expect to see coupling and thus the spectra taken from cavity one isn't shown. Cavity two, figures 7.1 & 8.1, resonates around the wavelength of the exciplex state, but does not show a Rabi splitting. Figure 8.1 shows the extracted peak locations of each peak shown in figure 7.1 for both polarizations of light.

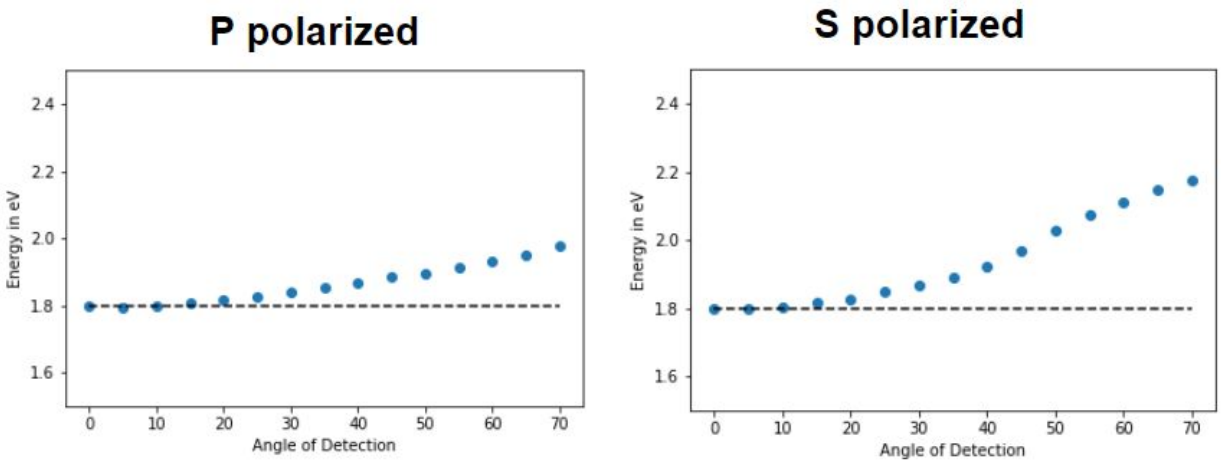

Figure 8.1: Extracted peak locations for cavity 2 shown in figure 7.1 graphed against angle of detection. Exciton energy is calculated by taking the central peak location of the exciplex emission from the uncovered film, see fig. 6.

One expects to see a curve matching the theoretical lower polariton curve shown in figure 4. This is not the case for cavity two. Polaritonic activity would have an asymptotic relationship to the exciton energy, unlike this cavity, which crosses through the exciton energy as a normal photon would. The exciton energy is roughly 1.8 eV, and we can see that the data passes through the exciton energy level. This value was calculated using the resonance wavelength shown in the table in section 3.2. This points to there being little to no interaction between the exciplex state and polariton creation.

Cavity three resonated across the wavelength of the excitation laser and thus is cut off. The peak locations are graphed along with the exciton and photon energy lines. Rabi splitting occurring in cavity three signifies that the molecule is still creating polaritons with the donor molecules, but not with exciplex states. Cavity three resonates around the wavelength of the donor molecule's Frenkel exciton's energy level. Here, the emission peak of the donor molecule's absorbance spectrum matches the wavelength that cavity three selects for.

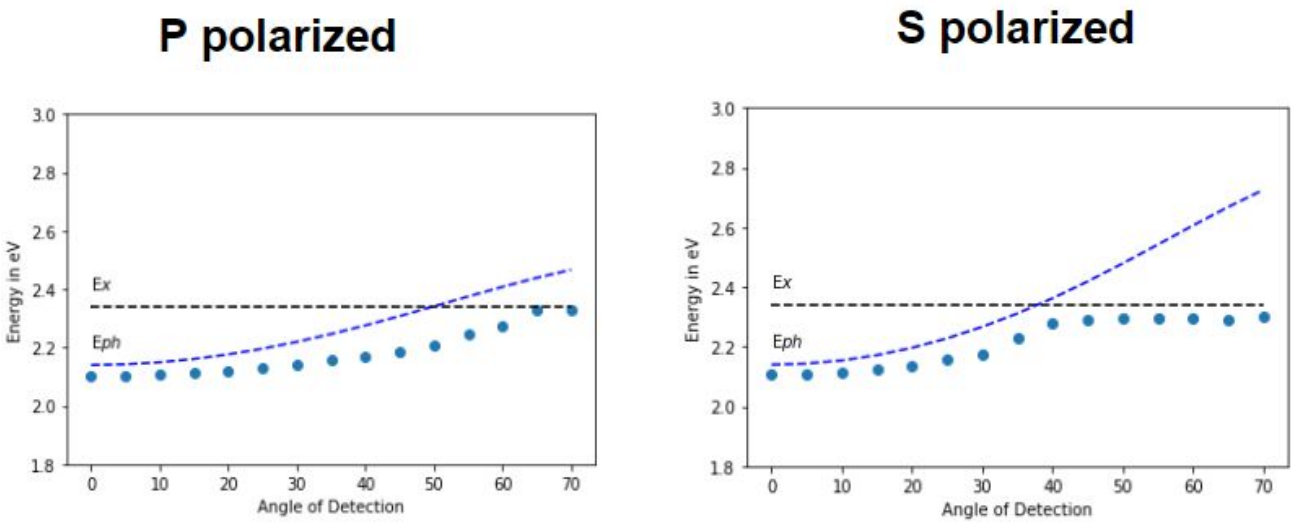

Figure 8.2: Peak locations in energy vs AOD for cavity 3. The exciton energy is again determined by the central peak location, this time of the isolated donor emission, roughly 530 nm, see fig. 6. Demonstration of Rabi splitting can be seen as the curve stops following the photon energy level and asymptotically approaches the exciton energy.

The exciton energy level for ADT-TES-F is roughly 2.34 eV and one can see the data matches the photon energy curve until it reaches the point of anti-crossing. A definite match in lineshapes shows that we are getting coupling between the Frenkel exciton of the donor in cavity 3. Rabi splitting was calculated using a curve fitting package in python. The Rabi splitting has been calculated to be ~200 meV and Rabi splitting in both the P and S polarizations are equivalent. This is consistent with previous publications that found a Rabi splitting of ~200-300 meV in cavities containing ADT-TES-F aggregates.[12] Rabi splitting has been shown to be proportional to concentration of aggregates, and the differences seen between the results of this thesis and our group's previous paper can be explained by this relationship. Further, differences seen between the effective index of refraction in S and P polarized measurements are also

similar. This all points to there being strong coupling with the donor's Frenkel exciton in cavity 3, and a lack of coupling to CTEs in cavity 2.

Conclusion:

4.1 Donor/Acceptor blends vs polariton creation

In conclusion, we have demonstrated experimentally a significant lack of polaritonic state creation in bulk-heterojunctions with CTEs. The organic blend of ADT-TES-F/ADT-TIPS-CN showed polaritonic activity in the range of the Frenkel exciton emission of the donor. Cavity two, that resonates in the range of emission of the CTEs, showed no confirmable signs of coupling. The third cavity showed Rabi splitting of ~200 eV in the emission peak location versus angle of detection shown in figure 8.2. The blend used in cavity creation was ninety eight percent donor and two percent acceptor, so the amount of CTEs emission is difficult to detect when the cavity is not selecting for the CTEs emission range. Further testing is required to determine any effects polariton creation has on CTEs creation rates. If the creation of polaritons can reduce CTEs creation, a large number of opportunities present themselves in new forms of CTEs reduction in devices.

Acknowledgements:

A special thanks to the NSF grant DMR-1808258 that funded this research.

Thanks to Prof. Minot for the use of his lab.

.

References:

[1] Liew, T.c.h., et al. “Polaritonic Devices.” Physica E: Low-Dimensional Systems and Nanostructures, vol. 43, no. 9, 28 Apr. 2011, pp. 1543–1568., doi:10.1016/j.physe.2011.04.003.

[2] Bulovic, Vladimir. “Excitons Excitons – Types, Energy Transfer.” *Https://Ocw.mit.edu/*, Massachusetts Institute of Technology, 27 Feb. 2003,

ocw.mit.edu/courses/electrical-engineering-and-computer-science/6-973-organic-optoelectronics-spring-2003/lecture-notes/7.pdf.

[3] Ostroverkhova, Oksana. *Handbook of Organic Materials for Electronic and Photonic Devices*. 2nd ed., Elsevier, Woodhead, 2019.

[4] Birks, JB "Excimers", *Rep. Prog. Phys.* **1975**, *38*, 903-974.

[5] Shepherd, W., Platt, A., Kendrick, M., Loth, M., Anthony, J. and Ostroverkhova, O. (2011). Energy Transfer and Exciplex Formation and Their Impact on Exciton and Charge Carrier Dynamics in Organic Films. *The Journal of Physical Chemistry Letters*, 2(5), pp.362-366.

[6] B. Rand, J. Xue, S. Uchida, and S. Forrest, "Mixed donor-acceptor molecular heterojunctions for photovoltaic applications. 1. material properties," J. Appl. Phys. 98, p. 124902, 2005.

[5] Katz, H.; Huang, J. Thin-Film Organic Electronic Devices. Annu. Rev. Mater. Res. 2009, 39, 71–92.

[6] Rani, V., Sharma, A., Kumar, P., Singh, B. and Ghosh, S. (2017). Charge transport mechanism in copper phthalocyanine thin films with and without traps. RSC Advances, 7(86), pp.54911-54919.

[7] Ellis, D. S.; Hill, J. P.; Wakimoto, S.; Birgeneau, R. J.; Casa, D.; Gog, T.; Kim, Young-June (2008). "Charge-transfer exciton in La_2CuO_4 probed with resonant inelastic x-ray scattering". *Physical Review B*. **77**: 060501(R).

[8] Polak, Daniel. "Manipulating Matter with Strong Coupling: Harvesting Triplet Excitons in Organic Exciton Microcavities." *ArXiv.org*, 2018, arxiv.org/ftp/arxiv/papers/1806/1806.09990.pdf.

[9] Ismail, Nur, et al. "Fabry-Pérot Resonator: Spectral Line Shapes, Generic and Related Airy Distributions, Linewidths, Finesses, and Performance at Low or Frequency-Dependent Reflectivity." *Optics Express*, vol. 24, no. 15, 2016, p. 16366., doi:10.1364/oe.24.016366.

[10] Haas, David. "Detection of Exciton Polaritons in Organic Thin Film TES-ADT." pp. 1–24.

[11] Shepherd, Whitney E. B., et al. "Aggregate Formation and Its Effect on (Opto)Electronic Properties of Guest-Host Organic Semiconductors." *Applied Physics Letters*, vol. 97, no. 16, 2010, p. 163303., doi:10.1063/1.3505493.

[12] Schenck, J. D. B. Van, et al. "Strong Exciton–Photon Coupling in Anthradithiophene Microcavities: from Isolated Molecules to Aggregates." *MRS Communications*, vol. 9, no. 3, 2019, pp. 956–963., doi:10.1557/mrc.2019.101.